Strong Coupling Theory for Superconducting Iron Pnictides

Wei-Qiang Chen,[1] Kai-Yu Yang,[2,1] Yi Zhou,[3] and Fu-Chun Zhang[1,4]

[1]*Department of Physics, and Center of Theoretical and Computational Physics, the University of Hong Kong, Hong Kong, China*
[2]*Institut fur Physik, ETH–Zurich, 8093 Switzerland*
[3]*Department of Physics, Chinese University of Hong Kong, Hong Kong, China*
[4]*Department of Physics, Zhejiang University, Hangzhou, China*

(Received 8 September 2008; published 30 January 2009)

Superconductivity in iron pnictides is studied by using a two-orbital Hubbard model in the large U limit. The Coulomb repulsion induces an orbital-dependent pairing between charge carriers. The pairing is found mainly from the scattering within the same Fermi pocket. The interpocket pair scatterings determine the symmetry of the superconductivity, which is extended s wave at small Hund's coupling, and d wave at large Hund's coupling and large U. The former is consistent with recent experiments of angle-resolved photoemission spectroscopy and Andreev reflection spectroscopy.

DOI: 10.1103/PhysRevLett.102.047006 PACS numbers: 74.70.Dd, 71.30.+h, 74.20.Mn

Superconducting (SC) iron pnictides have the highest transition temperature next to the cuprates [1–7]. The parent compounds are metallic spin density wave (SDW) states [8–11]. Superconductivity occurs when part of the Fe^{2+} ions are replaced by Fe^{+}. A multiorbital Hubbard model may be a starting point to study superconductivity [12–22]. Since the parent compound is metallic, most theories examine the SC instability from the weak Coulomb interaction point of view [13–18]. On the other hand, the observed magnetic moment in the SDW phase is large [23], indicating importance of spin couplings. The dynamic mean field theory [12] also suggests its closeness to a Mott insulator. This calls for an alternative approach from the viewpoint of large Coulomb repulsion U, which will be the purpose of the present Letter.

The electronic states of the compound are predominantly Fe-3d orbitals near the Fermi surface (FS) [10,11,24], which is composed of two hole pockets centered at $\Gamma = (0, 0)$ and two electron pockets at $X = (\pi, 0)$ and $Y = (0, \pi)$, in the unfolded Brillouin zone (BZ), corresponding to 1 Fe atom per unit cell. Note that the buckling of As atoms reduces the BZ to the square enclosed by the dashed lines in Fig. 1. The FS structure can be reproduced by a 5-orbital model [14]. The bands near the FS are mainly d_{xz} and d_{yz} orbitals [24], and the FS in the reduced BZ can be reproduced by a 2-orbital model, which shifts a hole Fermi pocket from the Γ- to the $M = (\pi, \pi)$ points in the unfolded BZ. In this Letter, we use the 2-orbital model to study the superconductivity at large U limit. We argue that our qualitative results will remain unchanged due to the simplification of the 2-orbital model. We find that the virtual hopping induces orbital-dependent pairings of charge carriers. The intra-Fermi pocket pair scattering is strongest, and the pairing symmetry is determined by interpocket pair scatterings and is extended s wave ($s_{\pm}$) for small Hund's coupling and d wave for large Hund's coupling and large U. The $s_{\pm}$- state was proposed by Mazin *et al.* [13] based on the analysis of the small Fermi pockets and spin fluctuations, and was found in weak coupling or small U approaches [14,15]. Our result appears consistent with the angle-resolved photoemission spectroscope (ARPES) [25] and Andreev reflection spectroscope [26].

The 2-orbital model reads [20] $H = H_0 + H_I$, where H_I is an on-site Coulomb term, and H_0 is a tight-binding model on a square lattice of Fe atoms,

$$H_0 = \sum_{\mathbf{k}nm\sigma} (\epsilon^{nm}_{\mathbf{k}} - \mu)\hat{c}^{\dagger}_{\mathbf{k}n\sigma}\hat{c}_{\mathbf{k}m\sigma} = \sum_{\mathbf{k}\alpha\sigma} \xi_{\mathbf{k}\alpha}\hat{c}^{\dagger}_{\mathbf{k}\alpha\sigma}\hat{c}_{\mathbf{k}\alpha\sigma}, \quad (1)$$

where $\epsilon^{nm}_{\mathbf{k}}$ is the hopping matrix in $\mathbf{k}$ space, $n = 1$ or 2 denote orbitals d_{xz} (or d_{yz}). μ is the chemical potential. $\alpha = \pm$ represents the electron or upper (+) band and the

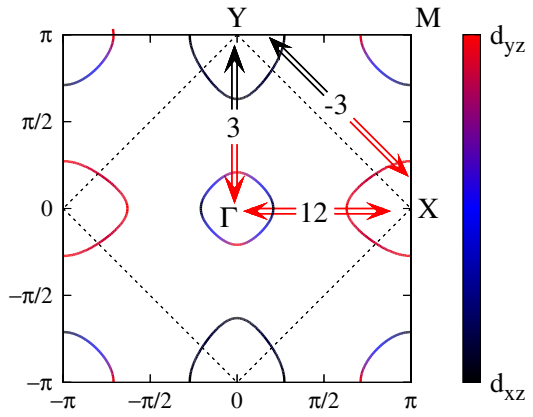

FIG. 1 (color online). Fermi surface in the unfolded Brillouin zone (BZ) of H_0. The square enclosed by the dashed lines is the reduced BZ. The color scheme illustrates weights contributed from orbitals d_{xz} and d_{yz}. Arrows indicate interpocket pair scatterings with wave vectors $\mathbf{q} \sim (0, \pi)$, $(\pi, 0)$, and (π, π). Numerics (positive value: attractive) are the corresponding scattering amplitudes $A^{mm}_{nn}(\mathbf{q})$ in Eq. (7) in unit of t^2/U at $J = 0$. Not shown is the intrapocket scattering $A^{nn}_{nn}[\mathbf{q} \sim (0, 0)] = 20t^2/U$.

hole or lower (−) band, corresponding to the diagonalized energy $\xi_{\mathbf{k}\pm}$. The band and orbital representations are related by a unitary transformation, $\hat{c}_{\mathbf{k}n\sigma} = \sum_{\alpha=\pm} u_{n\alpha}(\mathbf{k})\hat{c}_{\mathbf{k}\alpha\sigma}$. Here we follow Ref. [20] and parametrize H_0 by hopping integrals $t_{\vec{\tau}}^{nm}$ between two sites i and $j = i + \vec{\tau}$, which is the Fourier transform of $\epsilon_{nm}(\mathbf{k})$. We set $t_{\hat{x}}^{11} = t_{\hat{y}}^{22} = t_1$, $t_{\hat{y}}^{11} = t_{\hat{x}}^{22} = t_2$, $t_{\hat{x}\pm\hat{y}}^{nn} = t_3$, and $t_{\hat{x}\pm\hat{y}}^{12} = \pm t_4$ by lattice and orbital symmetry.

By choosing $t_1 = -t$, $t_2 = 1.3t$, $t_3 = t_4 = -0.85t$, the calculated FS with electron density per site ≈ 2.10 is reproduced in Fig. 1, which is similar to the first principle calculations [13,20] for LaFeAsO. The weight contributed from each orbital at the FS is illustrated in the figure. The state on the electron pocket around the X (Y) is mainly from d_{yz} (d_{xz}) orbital. The state on the hole pocket around the Γ consists of d_{yz} and d_{xz} orbitals equally if $\mathbf{k}$ is along the diagonals, and mainly from d_{xz} (or d_{yz}) orbital if along the x or y axis.

The on-site interaction

$$H_I = \sum_{i;m=1,2} [U\hat{n}_{im\uparrow}\hat{n}_{im\downarrow} + J\hat{c}_{im\uparrow}^{\dagger}\hat{c}_{im\downarrow}^{\dagger}\hat{c}_{i\bar{m}\downarrow}\hat{c}_{i\bar{m}\uparrow}] + \sum_{i;\sigma\sigma'} [U_{12}\hat{n}_{i1\sigma}\hat{n}_{i2\sigma'} + J\hat{c}_{i1\sigma}^{\dagger}\hat{c}_{i2\sigma'}^{\dagger}\hat{c}_{i1\sigma'}\hat{c}_{i2\sigma}] \quad (2)$$

where $\hat{n}_{im\sigma} = \hat{c}_{im\sigma}^{\dagger}\hat{c}_{im\sigma}$, U and U_{12} are the intra- and interorbital direct Coulomb repulsions, respectively. The terms with J are the exchange interaction. By symmetry, $U = U_{12} + 2J$. [27] In the limit, $U \gg t$, each lattice site is doubly occupied in the parent compound. Upon electron doping, some sites will have 3 electrons (or 1 hole). A single hole at site i may interchange with a two-hole state at site j, leading to a metallic phase. The effective interaction between two single holes on neighboring sites (i, j) can be derived by using second order perturbation theory, and it is given by

$$H_2 = -\sum_{ij}\sum_{nmn'm'} [A_{nm}^{m'n'}(ij)\hat{b}_{nm}^{\dagger}(ij)\hat{b}^{n'm'}(ij) + \sum_{S_z} B_{nm}^{m'n'}(ij)\hat{T}_{nm}^{S_z\dagger}(ij)\hat{T}_{S_z}^{n'm'}(ij)] \quad (3)$$

where $S_z = -1, 0, 1$, and

$$A_{nm}^{m'n'}(ij) = \left[\frac{(-1)^{m+m'}}{U-J} + \frac{1}{U+J}\right] t_{ij}^{nm} t_{ji}^{m'n'} + \frac{t_{ij}^{n\bar{m}} t_{ji}^{\bar{m}'n'}}{U_{12}+J}$$
$$B_{nm}^{m'n'}(ij) = \frac{(-1)^{m+m'}}{U_{12}-J} t_{ij}^{n\bar{m}} t_{ji}^{\bar{m}'n'}, \quad (4)$$

where $\bar{m}$ refers to the conjugate orbital of m, and the first and second terms in H_2 are the pairing interactions in the spin-singlet and triplet channels, respectively. The spin-singlet pair operator $\hat{b}^{nm}(ij) = (1/\sqrt{2})(\hat{c}_{in\uparrow}\hat{c}_{jm\downarrow} - \hat{c}_{in\downarrow}\hat{c}_{jm\uparrow})$, and the spin triplet pair operators T_{S_z} can be written similarly. In Eq. (3) and formalism hereafter, we use hole notation. The results plotted in all the figures, however, will be in the electron convention. Castellani *et al.* [27] studied the spin-spin coupling for a twofold orbital degenerate Hubbard model in the context of V_2O_3. Our expression here is equivalent to theirs, although the pairing forms were not explicitly given in their formalism. The spin triplet states become important at $J/U \to 1/3$, or $J \to U_{12}$, which can be seen clearly from the term in B. Below we focus on the spin-singlet state with even parity, which is energetically more favorable for J/U not so large. The pairing interaction between carriers derived in the large U limit should be relevant to the intermediate coupling region [28].

The effective Hamiltonian is then $H_{\text{eff}} = H_0 + H_2$, subject to the constraint of no more than 2 holes per site. This can formally be represented by a Gutzwiller projection operator to project all the unphysical states, similar to that in the t-J model [29]. H_{eff} may be studied by using a renormalized Hamiltonian approach to take into account the projection [30] by introducing renormalization factors, g_t for H_0 and g_2 for H_2, both are doping dependent. For a given doping, the effect of the renormalization is to scale all the $t's$ to $g_t t's$, and (U, J) to $(g_t^2/g_2)(U, J)$. Below we will absorb these renormalization factors into the parameters ($t's$ and U) and effectively set $g_t = g_2 = 1$ in our calculations.

H_{eff} can then be solved using a mean field theory by introducing mean fields for the spin-singlet pairing with even parity and symmetric orbitals [31], $\Delta_{nm}(\vec{\tau}) = \Delta_{mn}(\vec{\tau}) = \frac{1}{\sqrt{2}}\langle\hat{b}^{nm}(i, i+\vec{\tau})\rangle$, with $\vec{\tau} = \pm\hat{x}, \pm\hat{y}, \pm(\hat{x}\pm\hat{y})$. By symmetry, depending on $s_{\pm}$ (A_{1g}) or d wave (B_{1g}) states, we have $\Delta_{11}(\hat{x}) = \pm\Delta_{22}(\hat{y})$, $\Delta_{11}(\hat{y}) = \pm\Delta_{22}(\hat{x})$, $\Delta_{12}(\hat{x}) = \Delta_{12}(\hat{y}) = 0$, $\Delta_{11}(\hat{x}\pm\hat{y}) = \pm\Delta_{22}(\hat{y}\mp\hat{x})$, $\Delta_{12}(\hat{x}+\hat{y}) = -\Delta_{12}(\hat{x}-\hat{y})$. Note that $\Delta_{12}(\hat{x}\pm\hat{y}) = 0$ for the d wave state. The pairing strength with A_{2g} and B_{2g} symmetries [31] are found very tiny, and will not be discussed further [32]. The mean field Hamiltonian of H_{eff} can be written as

$$H_{\text{MF}} = \sum_{\mathbf{k}} \hat{\psi}_{\mathbf{k}}^{\dagger} \begin{pmatrix} \xi_{\mathbf{k}} & V(\mathbf{k}) \\ V^{\dagger}(\mathbf{k}) & -\xi_{\mathbf{k}} \end{pmatrix} \hat{\psi}_{\mathbf{k}}, \quad (5)$$

where $\hat{\psi}_{\mathbf{k}}^{\dagger} = (\hat{c}_{\mathbf{k}+\uparrow}^{\dagger}, \hat{c}_{\mathbf{k}-\uparrow}^{\dagger}, \hat{c}_{-\mathbf{k}+\downarrow}, \hat{c}_{-\mathbf{k}-\downarrow})$. $V(\mathbf{k})$ is a 2×2 matrix in band picture, given by

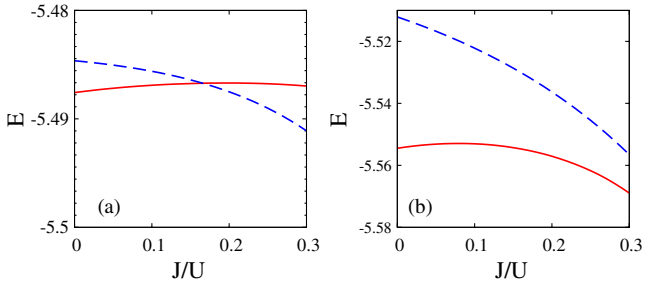

FIG. 2 (color online). Energy per site of H_{eff} in $s_{\pm}$ state (red solid line) and d wave state (blue dashed line) for (a) $t/U = 0.1$ and (b) $t/U = 0.2$.

$$V_{\alpha\beta}(\mathbf{k}) = \sum_{nmm'n';\tau} A^{m'n'}_{nm}(\vec{\tau})\Delta^{*}_{nm}(\vec{\tau})e^{i\mathbf{k}\cdot\vec{\tau}}u_{m'\alpha}(\mathbf{k})u_{n'\beta}(\mathbf{k}).$$

H_{MF} can be solved self-consistently, and the energy per site is $E = -\frac{1}{N}\sum_{\mathbf{k},\pm}E_{\pm}(\mathbf{k})$, with $E_{\pm}(\mathbf{k})$ the quasiparticle energy of the upper (+) and lower (−) bands, given by

$$E_{\pm}(\mathbf{k}) = \sqrt{w_{+}^{2} + V_{+-}^{2} \pm \sqrt{w_{-}^{4} + V_{+-}^{2}[(\delta\xi)^{2} + 4\bar{V}^{2}]}}, \tag{6}$$

where $\delta\xi = \xi_{+} - \xi_{-}$, $\bar{V} = [V_{++} + V_{--}]/2$, and $w_{\pm}^{2} = [\xi_{+}^{2} + V_{++}^{2} \pm (\xi_{-}^{2} + V_{-}^{2}{}_{-})]/2$, and the $\mathbf{k}$ dependence is implied. In Fig. 2, the energies of the SC states are depicted as functions of J/U for $t/U = 0.1$ and $t/U = 0.2$. At $t/U = 0.2$, the $s_{\pm}$ state is always energetically favorable. At $t/U = 0.1$, the ground state is $s_{\pm}$ wave if $J/U < 0.16$ and a d wave if $J/U > 0.16$.

In Fig. 3, we plot the intraband pairing amplitude $V_{++}(\mathbf{k})$ for the electron band and $V_{--}(\mathbf{k})$ for the hole band. In the $s_{\pm}$ state, $V(\mathbf{k})$ is invariant under a $\pi/2$ rotation, and $V_{++}(\mathbf{k})$ and $V_{--}(\mathbf{k})$ have a nodal line in the BZ. V_{++} have the same sign on X and Y pockets, but are opposite to V_{--} on Γ. In the d wave state, $V_{\alpha\alpha}(\mathbf{k})$ changes a sign under a $\pi/2$ rotation, and has nodal lines along the diagonals in the BZ.

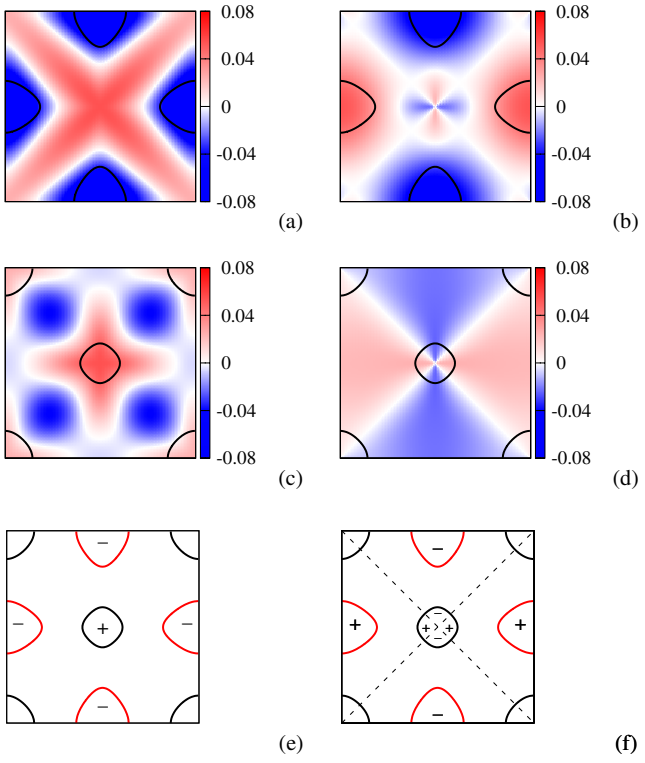

FIG. 3 (color online). Intraband pairing amplitude $V_{\alpha,\alpha}$ for $s_{\pm}$ (left) and d wave (right) symmetry states. Upper panels (a), (b) electron band, middle panels (c),(d) hole band. Fermi surfaces are indicated by the black lines. Lower panels (e), (f) relative sign of the pairing amplitudes and order parameters around Fermi pockets.

Let us examine the pairing strength at the FS around the Fermi pockets Y and Γ. For a Fermi wave vector $\mathbf{k_F}$ on the Fermi pocket centered at $C = (k_x^c, k_y^c)$, we define an angle $\theta = \arctan(k_y^F - k_y^c)/(k_x^F - k_x^c)$. The θ dependences of $V(\mathbf{k})$ are plotted in Fig. 4. For the $s_{\pm}$ state, $|V_{++}| \gg |V_{+-}|$, $|V_{--}|$ on Y pocket. This suggests that the SC pairing is mainly due to the electron pairing of the same orbital. At the pocket centered at Γ, V_{+-} is negligibly small, so that the SC pairing is mainly due to the hole pairings. We emphasize that although there are nodal lines, V_{++} on pocket Y and V_{--} on pocket Γ are always finite. The quasiparticle energy on the Fermi pockets are given by $E_{-}(\mathbf{k})$, which are shown in Fig. 4(e). There is a full gap on both Fermi pockets around Y and Γ, consistent with recent ARPES and Andreev reflection spectroscope results. Because of the above analyses, we have $E_{-}(\mathbf{k}) \approx V_{++}(\mathbf{k})$ around Y and $E_{-}(\mathbf{k}) \approx V_{--}(\mathbf{k})$ around Γ. The results for the d wave state are also shown in Fig. 4. The nodal line of $V_{--}(\mathbf{k})$ crosses the hole Fermi pocket and leads to a d wave like quasiparticle spectrum. The quasiparticle energy at the nodal point is given by $E_{\mathbf{k}} = V_{+-}^{2}(\mathbf{k})/E_{+}(\mathbf{k})$. Since $V_{+-}(\mathbf{k}) \neq 0$, but small, $E_{\mathbf{k}}$ is nonzero but very tiny [not distinguishable from 0 in Fig. 4(f)].

To better understand the SC pairing and its symmetry found above, we examine the pair scatterings in the orbital representation (intra- and interorbitals) near the Fermi pockets. The spin-singlet pairing interaction in H_2 can be written as

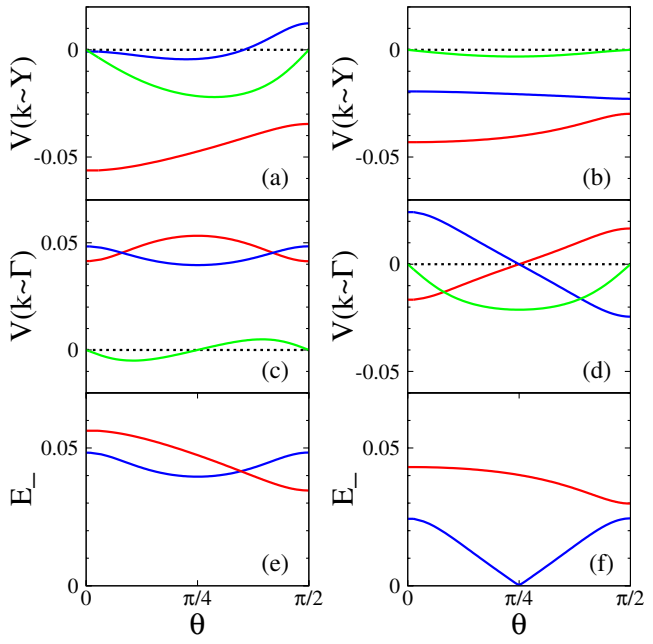

FIG. 4 (color online). Angle dependence of pairing amplitude $V_{++}(\mathbf{k})$ (red or gray line), $V_{--}(\mathbf{k})$ (blue or dark gray line), and $V_{+-}(\mathbf{k})$ (green or light gray line) along the Fermi pocket around Y (Γ) in the $s_{\pm}$-state [panel (a)/(c)] and the d wave state [panel (b)/(d)]. (e) and (f): the quasiparticle gap on the electron Fermi pocket (red or gray line) and hole Fermi pocket (blue or dark gray line) for $s_{\pm}$ and d wave states.

$$H_2^{\rm orb} = -\frac{1}{N}\sum_{\mathbf{k}\mathbf{k}',nmm'n'} A_{nm}^{m'n'}(\mathbf{q})\hat{b}_{nm}^{\dagger}(\mathbf{k})\hat{b}^{n'm'}(\mathbf{k}'), \quad (7)$$

with $\mathbf{q} = \mathbf{k} - \mathbf{k}'$, $\hat{b}^{nm}(\mathbf{k}) = (1/\sqrt{2})\langle \hat{c}_{\mathbf{k}n\uparrow}\hat{c}_{-\mathbf{k}m\downarrow} - \hat{c}_{\mathbf{k}n\downarrow}\hat{c}_{-\mathbf{k}m\uparrow}\rangle$. $A_{nm}^{m'n'}(\mathbf{q})$ is the Fourier transform of $A_{nm}^{m'n'}(ij)$. $H_2^{\rm orb}$ describes the pair scattering processes between two pairs of electrons with momentum $(\mathbf{k}, -\mathbf{k})$ and $(\mathbf{k}', -\mathbf{k}')$. Much of physics may be gained by examining the orbital diagonal term $\hat{b}^{nn}(\mathbf{k})$. Denote $\tilde{A}_{nn'}(\mathbf{q}) = A_{nn}^{n'n'}(\mathbf{q})$, with $\mathbf{q} = (q_x, q_y)$, we find

$$\tilde{A}_{11}(\mathbf{q}) = \frac{4U(t_1^2 c_x + t_2^2 c_y)}{U^2 - J^2} + \left(\frac{1}{U+J} + \frac{2}{U-J}\right)4t_3^2 c_x c_y,$$

$$\tilde{A}_{22}(\mathbf{q}) = A_{11}(q_y, q_x),$$

$$\tilde{A}_{12}(\mathbf{q}) = \frac{4}{U+J}t_3^2 c_x c_y - \frac{4J}{U^2 - J^2}t_1 t_2 (c_x + c_y), \quad (8)$$

where $c_x = \cos q_x$, $c_y = \cos q_y$, and we have set $t_4 = t_3$ for simplicity. Since we have small Fermi pockets, the pair scattering wave vectors are $\mathbf{q} \approx (0, 0)$ within the same pocket, and $\mathbf{q} \approx (\pi, 0)$ or $(0, \pi)$ between the pockets Γ and X or Y, and $\mathbf{q} \approx (\pi, \pi)$ between the pockets X and Y, as illustrated in Fig. 1. From Eq. (8), we find that the intrapocket pair scatterings are always attractive [$\tilde{A}(0, 0) > 0$], and strongest between the same orbital, and the pair scatterings between hole and electron pockets are always repulsive [$\tilde{A}(0, \pi) < 0$]. The pair scattering between the two electron pockets at X and Y points is mainly between two different orbitals, and $\tilde{A}_{12}(\pi, \pi)$ is attractive at small J/U, and repulsive at large J/U. This qualitatively explains the relative signs in the order parameters among the different Fermi pockets in both $s_{\pm}$ and d wave states as shown in Fig. 3. The scattering amplitudes in the case $J = 0$ are shown in Fig. 1, which is of $s_{\pm}$ symmetry.

We have used Eq. (7) and (8) to examine the effect to the superconductivity due to the simplification of the 2-orbital model, which results in the shift of a hole Fermi pocket from the Γ to M point. We have found that the qualitative physics obtained from our study of the 2-orbital model remains the same except the parameter space for the extended s wave state is enlarged when more accurate band structure is considered. To further ensure the qualitative conclusions of our theory, we have examined a 3-orbital model as in Ref. [18], in which there are two hole pockets around Γ in the unfolded BZ, which is better in agreement with the local-density approximation calculations. We have extended our analyses of Eq. (7) to that model and the pairing symmetries are found essentially the same as from the 2-orbital model.

In summary we have examined superconductivity in iron pnictides using a 2-orbital Hubbard model at the large U limit. An extended s wave pairing is found most stable in a large parameter space, consistent with early theories starting with weak coupling (small U) and with ARPES [25] and tunneling experiments [26]. Contrary to some of weak coupling theories, we find that the pairing is mainly from the pair scattering within the same Fermi pocket. Our analyses suggest some similarities between the superconductivity in iron pnictides and in the cuprates.

We wish to acknowledge the partial support from RGC grant of HKSAR and from Swiss National Foundation through the MANEP network.

[1] Y. Kamihara *et al.*, J. Am. Chem. Soc. **130**, 3296 (2008).
[2] X. H. Chen *et al.*, Nature (London) **453**, 761 (2008).
[3] G. F. Chen *et al.*, Phys. Rev. Lett. **100**, 247002 (2008).
[4] H. H. Wen *et al.*, Europhys. Lett. **82**, 17009 (2008).
[5] Z. A. Ren *et al.*, Europhys. Lett. **83**, 17002 (2008).
[6] M. Rotter *et al.*, Phys. Rev. B **78**, 020503(R) (2008).
[7] C. Wang *et al.*, Europhys. Lett. **83**, 67006 (2008).
[8] C. de la Cruz *et al.*, Nature (London) **453**, 899 (2008).
[9] M. A. McGuire *et al.*, Phys. Rev. B **78**, 094517 (2008).
[10] D. J. Singh and M. H. Du, Phys. Rev. Lett. **100**, 237003 (2008); K. Haule *et al.*, Phys. Rev. Lett. **100**, 226402 (2008).
[11] G. Xu *et al.*, Europhys. Lett. **82**, 67002 (2008); C. Cao *et al.*, Phys. Rev. B **77**, 220506(R) (2008); F. Ma and Z. Y. Lu, Phys. Rev. B **78**, 033111 (2008).
[12] K. Haule *et al.*, Phys. Rev. Lett. **100**, 226402 (2008).
[13] I. I. Mazin *et al.*, Phys. Rev. Lett. **101**, 057003 (2008).
[14] K. Kuroki *et al.*, Phys. Rev. Lett. **101**, 087004 (2008).
[15] F. Wang *et al.*, Phys. Rev. Lett. **102**, 047005 (2009).
[16] Z. J. Yao *et al.*, arXiv:0804.4166 [New J. Phys. (to be published)].
[17] Y. Ran *et al.*, Phys. Rev. B **79**, 014505 (2009).
[18] P. A. Lee and X. G. Wen, Phys. Rev. B **78**, 144517 (2008).
[19] X. Dai *et al.*, Phys. Rev. Lett. **101**, 057008 (2008).
[20] S. Raghu *et al.*, Phys. Rev. B **77**, 220503(R) (2008); X. L. Qi *et al.*, arXiv:0804.4332.
[21] Q. M. Si and E. Abrahams, Phys. Rev. Lett. **101**, 076401 (2008); J. H. Dai *et al.*, arXiv:0808.0305.
[22] G. Baskaran, arXiv:0804.1341; K. Seo *et al.*, Phys. Rev. Lett. **101**, 206404 (2008); M. M. Parish *et al.*, Phys. Rev. B **78**, 144514 (2008).
[23] H. Chen *et al.*, Europhys. Lett. **85**, 17006 (2009).
[24] L. Boeri *et al.*, Phys. Rev. Lett. **101**, 026403 (2008).
[25] H. Ding *et al.*, Europhys. Lett. **83**, 47001 (2008).
[26] T. Y. Chen *et al.*, Nature (London) **453**, 1224 (2008).
[27] C. Castellani *et al.*, Phys. Rev. B **18**, 4945 (1978).
[28] F. C. Zhang, Phys. Rev. Lett. **90**, 207002 (2003); J. Y. Gan *et al.*, Phys. Rev. Lett. **94**, 067005 (2005).
[29] P. W. Anderson *et al.*, J. Phys. Condens. Matter **16**, R755 (2004).
[30] F. C. Zhang *et al.*, Supercond. Sci. Technol. **1**, 36 (1988).
[31] Y. Zhou *et al.*, Phys. Rev. B **78**, 064514 (2008); Z. H. Wang *et al.*, arXiv:0805.0736; Y. Wan and Q. H. Wang, arXiv:0805.0923; J. R. Shi *et al.*, arXiv:0806.0259.
[32] M. Daghofer *et al.*, Phys. Rev. Lett. **101**, 237004 (2008). These authors reported B_{2g} ground state in the finite-size system study of the model with different parameters.